Tsugite: Interactive Design and Fabrication of Wood Joints

Maria Larsson, Hironori Yoshida, Nobuyuki Umetani, and Takeo Igarashi

The University of Tokyo

ma.ka.larsson@gmail.com, hyoshida@hy-ma.com, n.umetani@gmail.com, takeo@acm.org
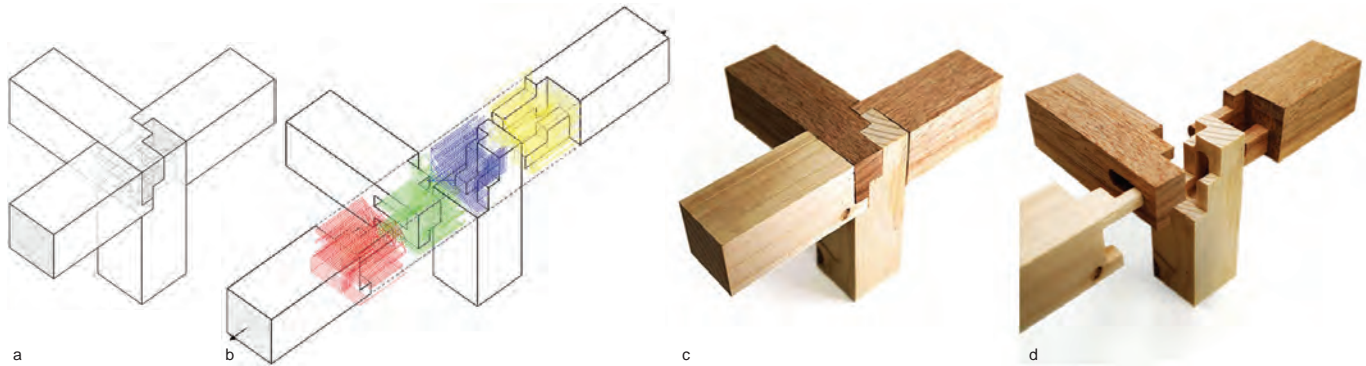
Figure 1. Connecting four timbers designed and CNC-fabricated using the Tsugite system. a) Interface screenshot of closed joint. b) Interface screenshot of open joint with a preview of milling paths. c) Fabricated joint closed. d) Fabricated joint open.

ABSTRACT

We present Tsugite—an interactive system for designing and fabricating wood joints for frame structures. To design and manually craft such joints is difficult and time consuming. Our system facilitates the creation of custom joints by a modeling interface combined with computer numerical control (CNC) fabrication. The design space is a 3D grid of voxels that enables efficient geometrical analysis and combinatorial search. The interface has two modes: manual editing and gallery. In the manual editing mode, the user edits a joint while receiving real-time graphical feedback and suggestions provided based on performance metrics including slidability, fabricability, and durability with regard to the direction of fiber. In the gallery mode, the user views and selects feasible joints that have been pre-calculated. When a joint design is finalized, it can be manufactured with a 3-axis CNC milling machine using a specialized path planning algorithm that ensures joint assemblability by corner rounding. This system was evaluated via a user study and by designing and fabricating joint samples and functional furniture.

Author Keywords

human–computer interaction; joinery; path planning; subtractive manufacturing; computer numerical control; computer-aided design; computer-aided manufacturing

CCS Concepts

•**Applied computing** → **Computer-aided design; Computer-aided manufacturing; •Computing methodologies** → Shape modeling;

INTRODUCTION

Traditional nail-free joinery connecting timber is a traditional craft. The technique is applied in architecture and for making furniture. Wooden joinery is appreciated because of its aesthetic appearance, high quality, and assemblability. There is a large variety of traditional joint geometries including dove tail, cross-lap, and scarf joints. These joint shapes tend to balance aesthetic and functional requirements. Designing and analyzing such joints is challenging because of the geometric complexity and criteria that need to be considered simultaneously. Further, crafting joints with hand tools is a slow and demanding process. Therefore, in this paper, we present an interactive system for creating wood joinery. The system analyzes a number of practical joint properties, and the joints are digitally fabricated by CNC-milling. We call the system Tsugite, from the Japanese word for joinery. The design space is a regularly spaced 3D grid, where each voxel belongs to a unique timber. This setup is suited for efficient computation, which enables real-time feedback, suggestions, and a combinatorial search.

The interface has two modes: manual editing and gallery. In the manual editing mode, the user directly manipulates the joint by pushing and pulling faces. When a block is added, the corresponding block on the mating timber is automatically subtracted, thereby ensuring that there are no overlapping or empty voxels. Further, the user receives real-time suggestions and graphical feedback about joint performance while modeling. The manual editing mode is appropriate for joint types

that have many solutions, and high-resolution joints for which a combinatorial search is not feasible because of the exponentially high number of possibilities. In addition, it is suitable for accommodating aesthetic criteria and other user-specified requirements. In the gallery mode, the user can browse and select among valid joints. This mode is convenient for difficult joints with few solutions and for nonexpert users.

The performance of a joint is evaluated based on eight metrics. Some of these metrics check for geometrically isolated parts and blocked sliding directions. These metrics are similar to those in previous works [2, 13, 14, 18]. We introduce new metrics to evaluate fabricability, durability, and friction and contact area. For fabricability, we analyze two properties: first, we test whether the geometry can be fabricated from a single direction, and second, we check for so-called "checkerboard patterns", which are problematic for fabrication and assembly. For durability, we observe that the strength of wood is 10–20 times higher in the fiber direction compared to its strength perpendicular to the fibers [12]. Therefore, protruding parts in nonfiber direction tend to break off. Tsugite analyzes the location of such parts to guide users to create durable joints.

Finally, when a joint design is finished, the system generates the tool path for 3-axis CNC fabrication. Our tool path algorithm identifies the location of the excess material in the inner corners where the cylindrical milling bit cannot reach, and rounds the corresponding outer corners of other timbers. The Tsugite system can be used for building wooden frame structures. This system enables anyone with limited expertise in joinery and with access to basic digital fabrication tools to create assemblies with sophisticated wooden joints. We ran a user study with an earlier version of the system and the result shows that the visual feedback reduces errors in the designs. The system presented in this paper is a refined version based on what we learned from the study. Finally, we show a number of joint samples and furniture designed using our system.

RELATED WORK

Interactive design of joints
Yao et al. propose a tool for designing free-form decorative joints [21]. The tool supports the design of ornamental joints with a high degree of geometrical freedom. However, it does not provide suggestions or feedback in real time. Further, the tool does not consider the fabrication constraints of a CNC machine. Most fabricated results are 3D-printed prototypes. They present a chair made from wood on a 1:1 scale, but it was reportedly handcrafted by a professional woodworker [21], which is time-consuming and costly.

Shape optimization of joints
Several recent works perform topological optimization of joints and 3D puzzles for interlocking and reconfigurable properties [2, 13, 14, 18]. Similar to our study, these works create joints within the design space of a 3D-grid of voxels. However, there is no user interface, and they do not consider practical constraints such as CNC fabricatability and durability with regard to the wood grain direction. The materialized results are mostly 3D-printed scale models or built with LEGO. Graphic results are occasionally rendered in wood, indicating a desire

to materialize the designs in wood. Wang et al. built a 1:1 scale chair by gluing wooden cubes together at the end of a wooden bar [18]. They demonstrated that their algorithm for the interlocking property works, but the apparent weakness of the joints does not result in usable furniture.

Interactive design of assemblies
Many other works propose computational systems for designing and fabricating assemblable structures. Some systems mill out joints from wood with a CNC machine [7, 15, 22], while others create bespoke joints using a laser cutter or a 3D printer [1, 4, 6, 10]. Further, some other authors propose methods for creating fabrication plans that can be executed using standard woodworking tools or standard tools in combination with digital fabrication machines [8, 19]. Another related work analyzes the physical validity of furniture and provides user suggestions while modelling [16]. To the extent that these works facilitate the creation of joints, the shapes are typically based on one or multiple standard joint shapes that parametrically adapt to various geometric conditions. For example, the joints adjust to various angles of the intersections and dimensions of the connecting pieces. The user can manipulate the global structure, but they cannot directly control the joint geometries in a meaningful way. Unlike these systems, we focus on designing the joint itself, rather than the global structure.

Digital fabrication of joints
Some works focus on joint geometries specifically adapted for CNC fabrication. Gros designed joint geometries appropriate for a 3-axis CNC machine and uploaded an online library with "50 Digital Wood Joints" for free use [3]. Kanasaki and Yang have similar ambitions to translate traditional Japanese joints into digitally fabricable shapes [5, 20]. However, their results are limited to only one or two joint geometries between no more than two orthogonally intersecting timbers. Note that these joints are designed so that there are no sharp inner corners to avoid the problem that the CNC machine cannot cut such shapes. Moreover, tool path planning for CNC milling has been studied since the 1970s. A tool path optimization problem is generally formulated as maximizing the volume of the removed material without cutting into the intended shape [11]. In our setup, it is necessary to cut into "the intended shape," i.e., to trim off sharp outer corners so that the mating timbers fit together. To the best of our knowledge, the problem of path planning for joinery with unreachable areas has not been considered previously.

Anisotropic materials
There are previous works that leverage the orientation of objects of anisotropic materials, i.e., materials with different properties in different directions. Li and Barbič propose a model for simulating the behavior of anisotropic materials such as wood, plants, and muscles [9]. Umetani and Schmidt [17] observe that for 3D printing with filaments, the layer-to-layer material bond in the z-direction is weaker than the continuous material bound in the xy-plane, and use this to optimize the object orientation accordingly. Unlike a 3D-printed object that has two strong and one weak axis, wood has only one strong axis, i.e., the direction of the fibers.

USER INTERFACE

The proposed system is implemented as a tool for designing a single wood joint for connecting timbers with rectangular sections. Figure 2 shows an overview of the workflow. The user specifies joint type variables including sliding axis, angle of intersection, and number of timbers (Figure 2a). This information comes from the overall design of the structure or furniture, which is beyond the scope of this work. In the manual editing mode, the user manipulates a geometry while receiving graphical feedback and suggestions (Figure 2b). In the gallery mode, the user can look through valid geometries and select one among them (Figure 2c). Finally, the Tsugite system considers the milling bit radius as an input, and exports the tool path to a CNC milling machine (Figure 2d).
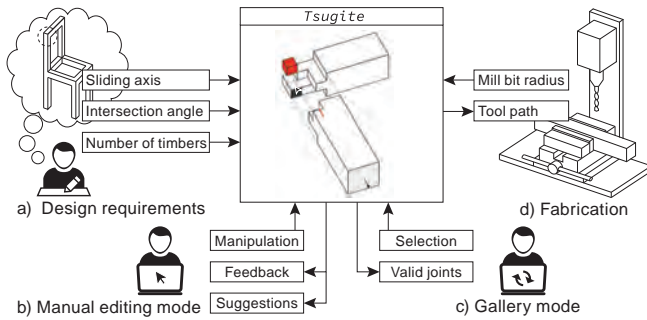

Figure 2. System overview.

Basic Operations

The user edits a joint by pushing and pulling on the faces in the sliding direction (Figure 3a). The user can further change the position and orientation of a timber by clicking and dragging its main body (Figure 3b and 3c). The user chooses an orthogonal sliding axis by pressing the x, y, or z key (Figure 3d). The system supports designs where all timbers slide along a single sliding axis, as in a stack. The number of intersecting timbers can theoretically be increased to six, thereby covering all sides of the cubic intersection (Figure 3e). However, the system is most suited for joints connecting four or fewer timbers because there are few or no solutions for 5–6 timber joints. The default voxel resolution ($3 \times 3 \times 3$) can be changed to one between 2 and 5 (Figure 3f). Finally, the user can set a nonorthogonal angle of intersection (Figure 3g), and the height and width of the cross-section of the timbers (Figure 3h).

Feedback

Tsugite provides visual feedback to the user based on the following eight performance metrics (Figure 4).

a) *Connectivity.* Voxels disconnected from the main body of the timber are shown in red.

b) *Bridging.* If a joint is located along the timber, there are cases where the joint geometry fails to bridge the two sides. If unbridged, separated sides are shown in two contrasting colors.

c) *Milling direction.* If there is no direction from which the joint geometry can be milled out, the body of the timber
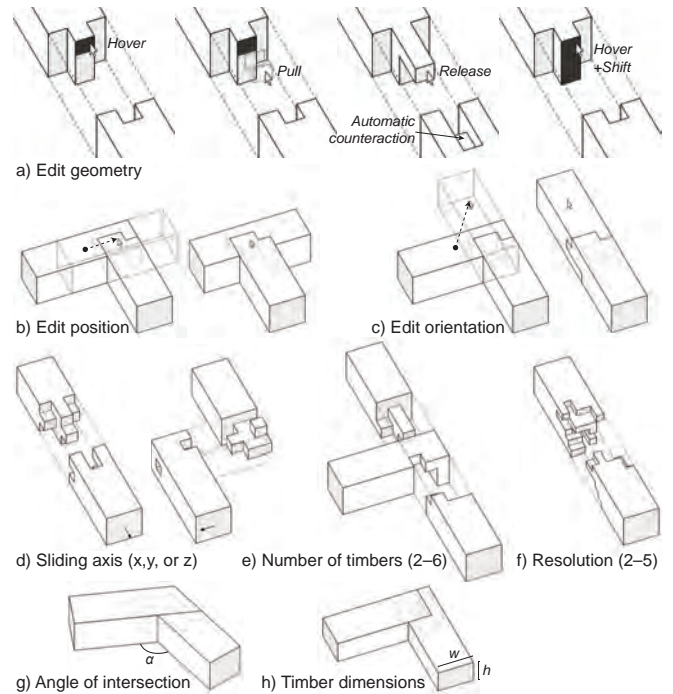

Figure 3. Mouse operations (a–c) and keyboard options (d–h).

is shown in orange. This failure mode occurs only for "sandwiched" timbers when there are three or more timbers in a joint.

d) *Checkerboard.* A prohibited checkerboard pattern is marked by a thick red vertical line in the center (see Implementation section for details about why this pattern is prohibited).

e) *Slidability.* Arrows at the end of each timber indicate all slidable directions of the current design. It is usually preferable for each timber to slide along the main sliding axis only. In the presence of undesired sliding directions, the outlines of that timber become red.

f) *Durability.* Nondurable voxels are shown in yellow. These voxels stick out perpendicular to the grain orientation, and therefore they tend to break off easily. Such parts are avoided in traditional joint geometries as well. A group of nondurable voxels is more fragile the further it sticks out and the smaller area of attachment it has. Our metric for durability is designed to provide lightweight feedback quickly; it is not a faithful evaluation of the structural strength of a joint such as that seen in finite element analysis (FEA).

g) *Contact area.* Contact area is the area where materials of different timbers touch each other. Such faces can be optionally previewed with a dotted texture. A larger contact area is preferred for joint intended to be glued.

h) *Friction area.* The friction area is the area that is under friction when the joint slides in and out. Such faces can optionally be previewed with a triangle texture. For joints intended to be held together by friction, a larger friction area is preferred. Note that we measure the *area* of the friction

and not the *force*. Analyzing the friction force would require physical testing and careful fine-tuning of parameters which is beyond the scoop of this work.

Metrics *a-f* are binary and *g-h* are numerical. A joint is valid if it meets the binary criteria. Valid joints can then be ranked according to the numerical criteria.
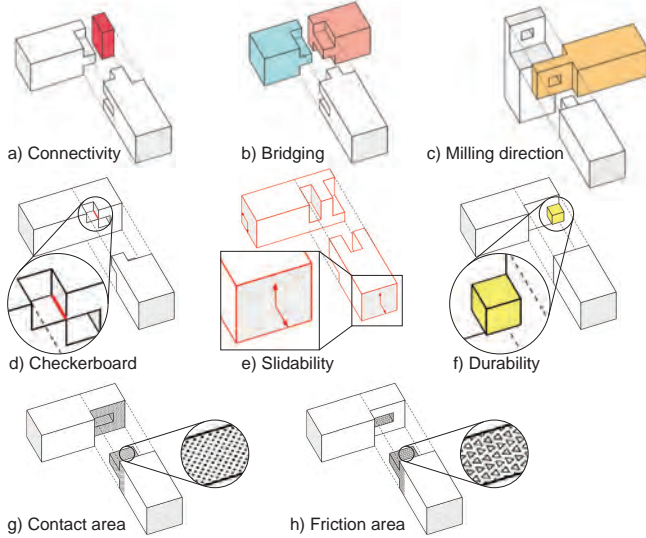

Figure 4. Graphical feedback.

Suggestions

If the current joint design is invalid, i.e., it fails to meet criteria *a-f* as formulated in the previous section, the system shows suggestions on the right side (Figure 5a). The suggestions consists of up to four valid joints within one edit distance from the current design, as ranked by a user-specified numerical criterion (friction or contact area). When the user hovers over a suggestion, the difference between the current design and suggestion is displayed on top of the current design. An added or subtracted voxel is shown with dashed outline and white or red filling, respectively. A suggestion is adopted by clicking on it.

Gallery

Sometimes, it is difficult for the user to find a valid joint by manual editing, whether it is because of a lack of experience or that the particular joint type has very few possible solutions. Therefore, the system offers the gallery mode. In this mode, the user can browse among pre-calculated valid geometries, viewing up to 20 geometries at once, and select a desired one (Figure 5b). Similar to the suggestions, the valid joints are optionally ranked according to friction or contact area. The gallery mode is provided for joints with a resolution up to $3 \times 3 \times 3$. For higher resolutions, there are too many combinations to run through all possibilities.

Fabrication

After finalizing a design, the user can preview the milling path (Figure 6) and export it to a CNC machine. To fabricate a joint, the user fixes the material in the bed of the CNC machine, sets the machine origin, and runs the machine.
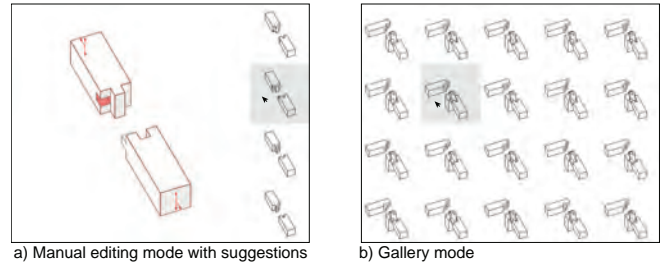

a) Manual editing mode with suggestions   b) Gallery mode

Figure 5. Interface modes.

Tool path display   *Perspective view*   *Top view*
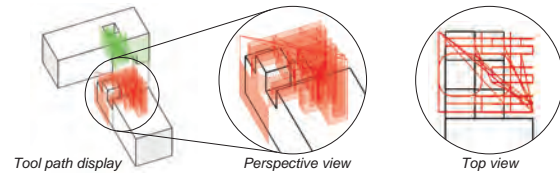
Figure 6. Milling path display.

IMPLEMENTATION

The system defines and enforces geometric constraints for fabrication using a 3-axis CNC machine. We present an efficient data structure and a number of functions for analyzing the geometric performance. Further, we propose a path planning algorithm that ensures joint assemblability by corner rounding. The system was implemented in Python with OpenGL and GLFW as main dependencies.

Fabricability

The geometric criteria for joinery vary based on the fabrication method. We limit ourselves to fabricating joints with a 3-axis CNC machine equipped with a standard milling bit because of its affordability and popularity. This machine setup poses two major constraints. First, it is not possible to cut sharp inner corners parallel to the milling bit (Figure 7a). Such corners have a round fillet with the radius of the milling bit. Second, the machine can approach the material only from above. This means that the machine cannot fabricate a geometry that needs to be cut out where the access from above is blocked (Figure 7b).
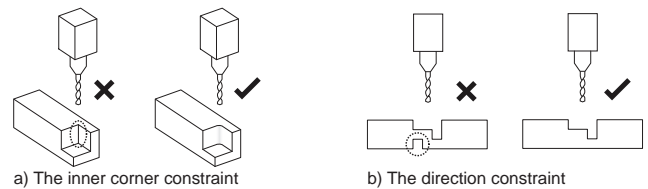

a) The inner corner constraint   b) The direction constraint

Figure 7. Fabricability constraints for 3-axis CNC milling.

The inner corner constraint (Figure 7a) has two implications for the system. The first problem appears if we attempt to fabricate a voxelized geometry with a conventional path planning tool that considers each timber of the joint individually. In this case, it will not be possible to assemble the pieces because the surplus material of the inner corners of one timber will collide with the corresponding sharp outer corners of another timber (Figure 8a). There are two common solutions to this problem: removing more material from the inner corners (Figure 8b) or

rounding the outer corners (Figure 8c). Both these strategies are observed in existing digital joints. We chose the second solution (rounding of outer corners) because it does not have any air pockets, which looks nicer and provides more friction area and strength. Automating corner rounding is the key function of our specialized path planning algorithm (see the section Path Planning for details).
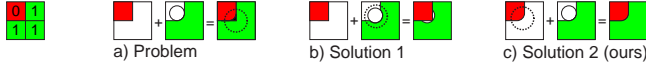

Figure 8. a) Problem of conventional path planning: the joint is unassemblable. b-c) Possible solutions.

The second consequence of the inner corner constraint (Figure 7a) is nonobvious; it makes checkerboard patterns problematic. The reason should become clear by reviewing the alternative rules in Figure 9. If we allow checkerboard patterns without additional rules, the timbers will be impossible to assemble (Figure 9a). An alternative rule would be to round the corners of one timber like outer corners (Figure 9b). However, the gap (d) between the two protruding parts of the second timber will be narrower than the diameter of the milling bit. Therefore, it cannot be fabricated. A third possibility would be to increase this gap until the milling bit can pass through (Figure 9c). In this case, the geometry can be fabricated and assembled. However, it is still not a satisfactory solution because it adds complexity to the system (the user would need to decide which timber to apply which rule to). Moreover, it removes a considerable amount of material on one side compared to the other, which in the case of neighboring checkerboards can result in narrow parts where the milling bit might not reach (Figure 9d). Therefore, we chose to prohibit the checkerboard pattern altogether.
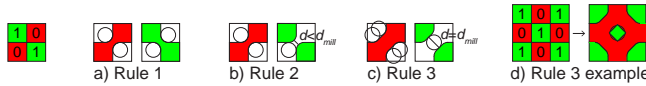

Figure 9. Alternative unsatisfactory rules for checkerboard patterns.

The direction constraint (Figure 7b) introduces the limitation that each timber is milled from a single fabrication direction. This means that fabricable geometries are limited to those that can be expressed as a height field. This observation is the basis for the data structure (refer to the next section).

Furthermore, a joint fabricated using a single fabrication direction is always slidable in that direction (Figure 10a). To simplify the problem by leveraging this property, we impose the limitation that there is only one sliding axis for all timbers of a joint (like in a stack), and that the fabrication and sliding axes are shared. In this situation, it is possible to find fabricable geometries where only two pieces (the first and last) slide out in the assembled state (Figure 10b). The definition of the interlocking property is that only *one* piece should be movable in the assembled state. Therefore, a valid joint in the Tsugite system is never interlocking by itself (it has *two* movable pieces). However, it is possible to arrange the joints in a global assembly with interlocking property, as demonstrated by the interlocking stool in the Results section (refer to Figure 23).
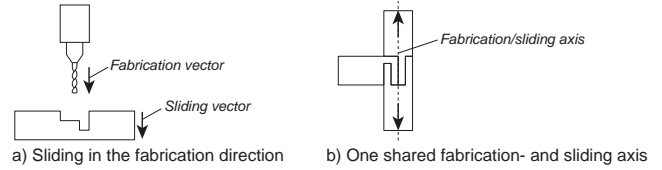

Figure 10. Fabrication direction implications.

Data Structure

Internally, a joint is represented by a 3D matrix of integers, where each integer indicates a unique timber ID. As discussed in the previous section, the design space is limited to geometries that can be expressed as a height field. By initializing the geometry as a 2D height field, the number of possibilities is greatly reduced, compared to the entire design space of a 3D cube of voxels. In the case of a $3 \times 3 \times 3$ resolution joint between two timbers, the number of possible designs are reduced from about 134 million to about 260 000 (Figure 11). For joints with a higher resolution or more intersecting timbers, the number of possibilities increase exponentially.

$27^{27} = 134\ 217\ 728$ $4^9 = 262\ 114$ (ours)

Figure 11. For a two-timber joint in $3 \times 3 \times 3$ resolution, the number of possibilities for a voxelized cube (left) compared to the height field representation (right).

The first height field is given as a 2D matrix of integers ranging from zero to the maximum height given the resolution. This height field describes the distribution of voxels between two timbers. When there are more than two timbers, additional height fields are added to describe the distribution between each sequential pair. Oblique and nonsquare joints have the same data structure; these variables are accommodated by the deformation of the 3D-grid (Figure 12). Finally, it is necessary to consider which of the six sides of the joint are connected to the main body of the timber. We refer to these as "fixed sides." In our implementation, each timber has either one or two fixed sides. One fixed side indicates that the joint is located at the end of a timber, which is the case for the timbers of an L-joint. Two fixed sides means that the joint is located somewhere in the middle of the timber, as for the timbers of an X-joint.
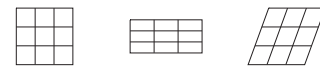

Figure 12. Grid distortion principle to accommodate nonsquare timbers and nonorthogonal angles of intersection.

Joint Performance Analysis

The eight feedback metrics are calculated as follows.

a) *Connectivity.* We run a flood fill algorithm starting from all fixed sides of a timber, and determine whether it covers all voxels belonging to the timber. Covered voxels are connected; and uncovered voxels are unconnected.

b) *Bridging.* Bridging is evaluated for timbers with two fixed sides. We run a flood fill algorithm starting from one fixed

side of the timber. If it includes any voxel adjacent to the second fixed side, the joint is bridged.

c) *Milling direction.* When there are more than two timbers, we verify that the middle timbers can be fabricated. A middle timber needs to be milled from one of the two directions along the sliding axis (from top or bottom). The system automatically finds an appropriate milling direction. If it is necessary to mill the middle timber from both directions, the geometry is identified as invalid.

d) *Checkerboard.* For all interior vertices, we analyze the four neighbors in the plane perpendicular to the fabrication axis. A checkerboard pattern is identified when there are two crossing diagonals (Figure 13a). If there is only one diagonal, and the other two voxels belong to different timbers, it is *not* a checkerboard pattern (Figure 13b). We call this second instance an "apparent" checkerboard pattern. For examples of joints with true and apparent checkerboard patterns, refer to Figure 30.
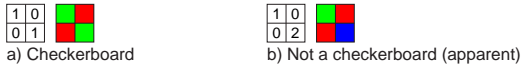

Figure 13. Checkerboard pattern analysis.

e) *Slidability.* Each of the six orthogonal sliding directions is evaluated separately. For each timber ID, and for each column of voxels aligned with the direction currently being tested, we check if there is an instance of the *same* ID after an instance of a *different* ID in that direction. If this is true anywhere, these voxels collide, thereby preventing the timber to slide in that direction.

f) *Durability.* We identify a timber of a joint as nondurable when a plane parallel to the fiber axis separates the timber into two connected components, where one is connected to a fixed side and the other is not (Figure 14).

g) *Contact area.* For each timber, we calculate the sum of the area of exterior faces adjacent to other timbers (Figure 15a). By the principle "a chain is not stronger than its weakest link," the slidable timber with the least contact area represents the contact area of the joint when ranking valid joints.
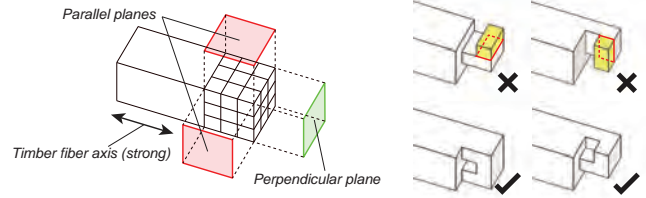

Figure 14. Durability analysis.

h) *Friction area.* For each timber, we calculate the sum of the area of exterior faces adjacent to other timbers *and* those that are not in a plane perpendicular to any unblocked sliding direction (Figure 15b). By the same principle as for the contact area, the slidable timber with the least friction area represents the friction area of the joint.
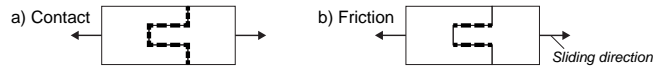

Figure 15. Contact and friction area analysis.

Search

For the suggestions, we search for valid geometries within one edit distance from the current design. This can be calculated in real time. For the gallery mode, we pre-calculate valid geometries for each joints type. Table 1 lists the number of valid joints and the occurrence of failure modes for all seven unique two-timber joints types. We run through all 262 144 (4^9) geometries in the default $3 \times 3 \times 3$ resolution. Our assumption was that perpendicular I- and L-joints *always* have nondurable parts because some part needs to "stick out" perpendicular to the grain to prevent sliding in the axial direction. However, the combinatorial search found a few joints that avoid this failure mode. For examples of those geometries, refer to Figure 24b and 24d.

For joints connecting more than two timbers, we employ the strategy to cut branches early on to avoid the exponential growth of possibilities. We start by producing all valid geometries for only one timber of the joint. Then, for each valid geometry of the first timber, we divide the remaining voxels between the remaining timbers. To further help cutting branches early on, we add the constraint that each timber should have at

Table 1. Occurrence of failure modes and valid two-timber joint geometries for all unique joint types and all 262 144 (4^9) geometries with the $3 \times 3 \times 3$ resolution. We consecutively removed the failure modes from the top to the bottom.

		I-axial	I-perp	L-axial	L-perp	T-axial	T-perp	X-perp
	Total	262,144	262,144	262,144	262,144	262,144	262,144	262,144
a)	Connectivity	-0	-99,152	-52,884	-99,690	-7,083	-59,046	-7,083
b)	Bridging	-0	-0	-0	-0	-35,146	-31,864	-54,829
c)	Milling direction	-0	-0	-0	-0	-0	-0	-0
d)	Checkerboard	-145,608	-68,822	-104,020	-68,390	-114,494	-76,986	-104,864
e)	Slidability	-28,028	-19,114	-20,500	-13,506	-13,691	-6,870	-0
f)	Durability	-0	-74,872	-76,358	-80,504	-23,622	-84,166	-25,214
	Valid	88,508	184	8,382	54	68,108	3,212	70,154

least three voxels to be valid. This is a reasonable constraint because a timber attached by fewer than three voxels does not make a very good joint. With this method, we can search through all possibilities for the $3 \times 3 \times 3$ joints connecting three and more timbers (with the exception of joints with considerably many possibilities for which we stopped the search at 1 million valid joints). We found valid geometries for some instances of 3- and 4-timber joints (Table 2). For 5- and 6-timber joints, there are no solutions in the default resolution (although solutions might exist for higher resolutions joints). Running through a two-timber joint took 30 min, and each 3- to 6-timber joint took 3–9 h. We used a desktop computer with a 3.7 GHz CPU.

Table 2. Number of valid geometries for instances of 3-timber joints with the $3 \times 3 \times 3$ resolution.

	3-tim a	3-tim b	3-tim c
Valid	1,000,000+	40,452	913

Path Planning

The tool paths are generated directly from the three-dimensional binary matrix of each timber. A joint is milled out layer by layer, starting with the top layer of voxels. First, a void region is detected (Figure 16a). A void region is an area of connected voxels that should be removed. We create a finishing path following the material surrounding the void region with an inward offset (Figure 16b). The center of the milling bit will travel along the path and remove the material on both sides as per the lengths of its radius. Therefore, the path is offsetted from the edge of the material by the radius of the milling bit.

a) Void region   b) Finishing   c) Rounding   d) Roughing   e) Tool path

Figure 16. Milling path generation.

Then, the outer corners of the finishing path are conditionally rounded (Figure 6c). This is the key function of the algorithm that ensures joint assemblability. An outer corner is rounded when it is located on the inner corner of a mating timber, i.e., two adjacent void cells are occupied by a common timber (Figure 17a). Otherwise, if the two adjacent void cells are occupied by different timbers, the corner remains sharp (Figure 17b). For an example of selective corner rounding, we refer to Figure 29. The amount of the fillet depends on the size of the milling bit, as demonstrated in Figure 28. After creating the finishing path, areas of the void region that are *not* covered by the finishing path are additionally cut with a co-linear oscillated roughing path (16d). The final tool path for the void region combines the finishing and roughing paths (16e). Then, the algorithm goes on to the next region, and then to the next layer, until all void voxels are covered.

The generated tool path is exported in the G-code format where the path is composed of lines and circular interpolations.
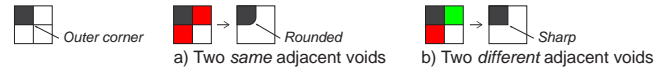

Outer corner   →   *Rounded*   →   *Sharp*
a) Two *same* adjacent voids   b) Two *different* adjacent voids

Figure 17. Conditional rounding of outer corners.

The G-code file contains the full machine instructions, and it can be loaded into a G-code interpreter software that directly controls the CNC machine. The speed and layer depth are set to standard values, and they can be manually adjusted for particular types of wood such as hard or soft wood.

Material positioning for fabrication

To fabricate a joint, the user needs to position the timber correctly. When the fabrication direction is aligned with the axis of the timber, it is inserted vertically (Figure 18a). Otherwise, the timber is inserted horizontally, so that the axis of the timber is aligned with the *x*-axis of the CNC machine (Figure 18b). Furthermore, the center point on the top of the joint corresponds to the machine origin. To reference this point, the user draws a cross, manually moves the milling bit to the center of the cross, and sets the machine origin there. Depending on the type of CNC machine and the length of the timber, it might not be possible to insert the timber vertically. In such cases, the user is limited to designing joints with nontimber-axial sliding.
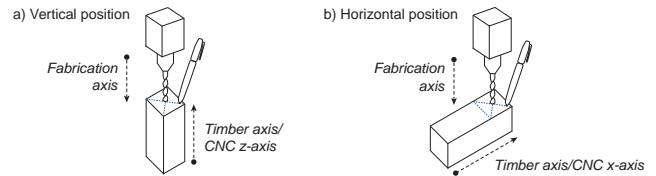

a) Vertical position   b) Horizontal position

Fabrication axis   *Timber axis/ CNC z-axis*   *Fabrication axis*   *Timber axis/CNC x-axis*

Figure 18. Positioning the timber vertically (a) or horizontally (b), and setting the machine origin.

USER STUDY

We ran a user study with an earlier version of our system to confirm the effectiveness of the visual feedback and to obtain insights for further improvements. We later made additional improvements to the system such as making feedback clearer, and adding suggestions and the gallery mode.

Setup

We recruited volunteer participants among our colleagues. In total, 20 people participated (6 women and 14 men). Their background was in computer science (75%) or architectural design (25%), and most were between 20 and 40 years old (95%). About half of the participants had little or no experience with 3D modeling (60%). We asked each participant to perform two tasks, to design the joints for a chair. Contact and friction feedback were not implemented yet. The first task was an axial I-joint. It is relatively easy to design because there are many solutions. Possible failure modes are checkerboard and slidability. The second task was an axial L-joint. It is more challenging since it has more failure modes and fewer valid solutions. Every other participant performed the tasks with or without graphical feedback. First, the participants were given up to 5 min to familiarize themselves with the interface while receiving a tutorial. Second, for each task, we explained the

failure modes, and then they had up to 5 min to complete their design. When finished, the geometry was saved with a time stamp. After each task, the participants were asked to fill out a questionnaire about their experience with the software. Last, the participants in the group without feedback were allowed to test the interface with feedback, and vice versa. Then, they answered one last question that compared the two feedback modes.

Results

Figure 19 shows the designs created by the participants. The designs are diverse and unique, apart from the four instances of the I-axial joints with plus-shaped geometry. Table 3 summarizes the quantitative results of the two groups. When we sum up all errors, the group with feedback performed better than the group without; the total error count was 8 for the group with feedback, compared to 13 for the group without feedback (Table 3). Yet, the number of errors for the group with feedback was surprisingly high. We see that most errors were due to durability failure, which is relatively difficult to resolve. If we exclude this error, the error count is only 1 for the group with feedback (Table 3). For the question what was the most difficult, the participants in the group without feedback reported that it was difficult to assess nondurable voxels (50%) and checkerboard patterns (30%). For the question about suggestions for interface improvements, three participants in the group without feedback suggested some form of graphical feedback. After testing the interface in the other feedback mode at the end, every participant preferred the interface with the feedback. They stated that it was "much easier," "helpful," and "necessary." One participant without feedback stated "It was hard and laborious to check if the joint met criteria each time I changed the design." Furthermore, six participants suggested some physical simulation to help assess the structural strength of their designs. Two participants proposed increasing the design space; they would have liked to control the proportions of the voxels and design angled dovetail joints.

Table 3. Quantitative results from the user study showing that the groups with feedback had a lower error count.

	N	Time ave.	Errors	Errors except durability
Feedback	10	2 min 18 s	8	1
No feedback	10	2 min 53 s	13	8

Lessons Learned

From the user study, we learned that visual feedback is helpful for the user to spot a problem; however, it does not necessarily help the user to find a solution. In particular, it was difficult for some participants to resolve the durability error. Based on this observation, we implemented suggestions and the gallery mode to support users to more easily find valid joints. Furthermore, we made the durability feedback clearer. In the earlier version, this was marked by a dashed yellow outline. It was difficult to notice and it did not look alarming, which might have contributed to this error remaining untreated. Finally, in the earlier version slidability was shown by arrows only. One person in the group with the feedback missed this error, supposedly because visual attention is on the joint geometry itself, rather than the bottom edge of the component where the
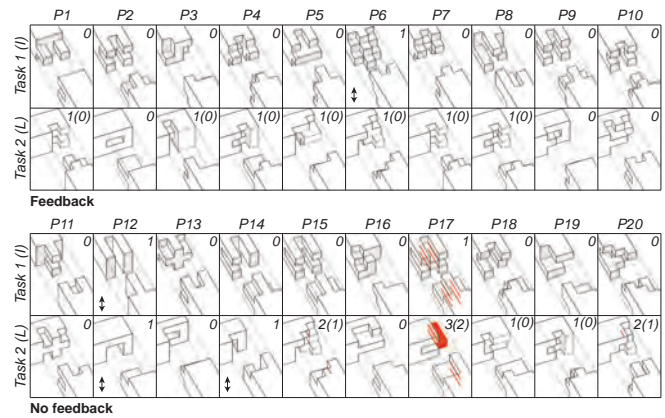

Figure 19. Designs created by participants in the user study for the groups with feedback (*P1–P10*) and without feedback (*P11–P20*). The numbers in the upper right corners are the total error count for the current design. The number within parenthesis shows the error count without counting the durability error.

arrows are displayed. Therefore, we added a visual clue for the slidability error—when a timber is sliding in an undesired direction, its outline becomes red.

RESULTS

Assemblies

To demonstrate the usefulness and capability of the system, we show the functional furniture and other assemblies that are fabricated or presented as graphics. Figure 20 shows a chair fabricated with the system. It has nine joints: five 2-timber joints and four 3-timber joints. The joints are held together by friction only and the chair is stable enough for a person to sit on it. Figure 21 shows a table with 14 joints including L-, oblique T-, and X-joints. Figure 22 shows "UIST" written with four I-joints. The joints were designed in the manual editing mode and some are actually not fully valid in the Tsugite system because of the durability error. However, to create the letters, this criterion was deemed secondary. Figure 23 shows the design of an interlocking stool with eleven timbers connected by four 3-timber joints and six 2-timber T-joints. Furthermore, all joints of the stool are unique, and therefore there is only one way in which it can be assembled.

Figure 20. Chair fabricated from 12 timbers connected by nine nail-free and glue-free joints.

Figure 21. Table fabricated from 10 timbers connected by 14 nail-free and glue-free joints including four oblique ones.
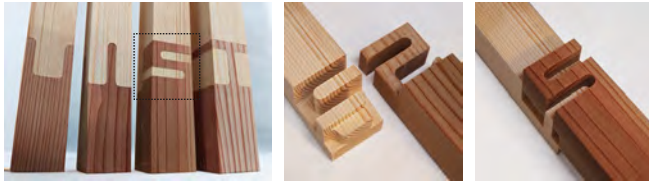

Figure 22. UIST written with four fabricated I-joints.

Figure 23. Interlocking stool assembly with eleven pieces connected by four unique 3-timber joints and six unique two-timber T-joints.

Joint Samples

To demonstrate various joint types, parameters, and technicalities, we designed and fabricated a number of samples. We fabricated examples of joints with all unique orientations and positions of 2-timber joints (Figure 24). Further, we fabricated joints with 3 and 4 intersecting timbers (Figure 25). These were designed by selecting joints in the gallery mode and then adding some manual edits. To test other resolutions, we designed and fabricated joints in the nondefault settings. For the lowest resolution of $2 \times 2 \times 2$ there are very few possibilities and few valid joints (Figure 26a). For the highest resolution of $5 \times 5 \times 5$, we can create joints with high variety and high friction, although it was a bit tedious to model with many faces (Figure 26b). Further, we fabricated a 4-timber joint in a $4 \times 4 \times 4$ resolution (Figure 1). To design this joint, we could not use the gallery mode because of the high resolution. However, we managed to manually design this joint by employing geometrical strategies observed in the valid results the 3-timber joint searches. The geometrical strategy was to avoid nondurable parts by creating holes in the middle timbers. In addition, we demonstrated the angle of intersection parameter by fabricating an oblique joint (Figure 27a), and the height and width dimension parameters by fabricating a joint from timbers with nonsquare sections (Figure 27b).

Further, we fabricated a series of joint samples to demonstrate technicalities of the fabrication: corner rounding and checkerboard pattern. To show how the milling bit affects the joint geometry, we fabricated a pair of identical joints with different milling bit diameters (Figure 28). The fabricated
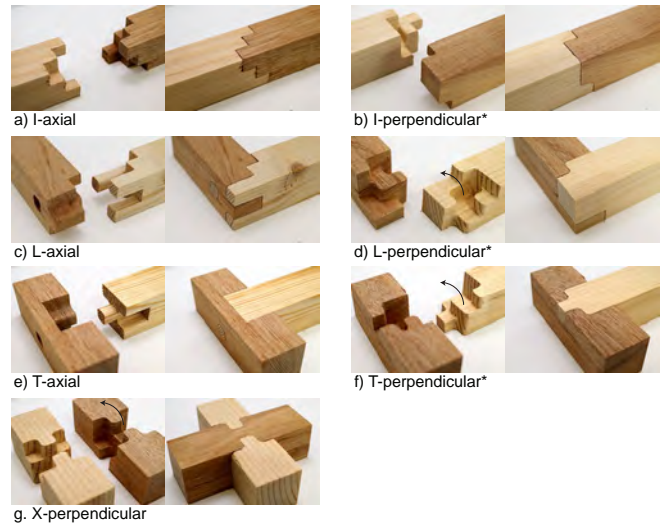

a) I-axial   b) I-perpendicular*

c) L-axial   d) L-perpendicular*

e) T-axial   f) T-perpendicular*

g. X-perpendicular

Figure 24. All 7 unique 2-timber joint types. *Created with gallery mode.

a) 3-timber joint*   b) 4-timber joint*
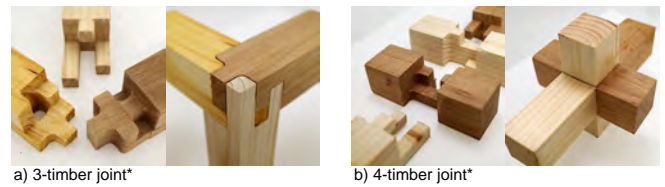
Figure 25. 3- and 4-timber joints.

a) 2×2×2   b) 5×5×5

Figure 26. Nondefault resolution joints.

a) 105 degree intersection   b) 44 × 24 mm section
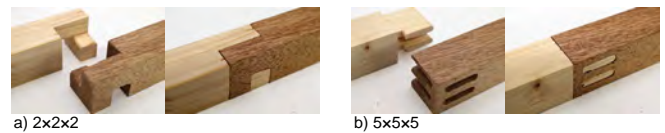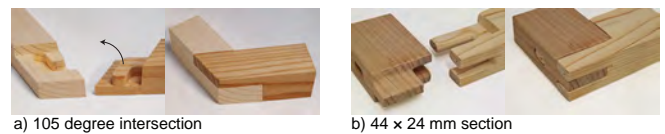
Figure 27. Nonorthogonal and nonsquare joints.

geometries have different radii of the rounded fillets of the inner and outer corners. To demonstrate the selective rounding of outer corners by the path planning algorithm, we fabricated a pair of 2- and 3-timber joints with the same geometry of the first timber (Figure 29). The outer corners of the first timbers were rounded differently because of the different local conditions. Finally, we fabricated one obvious checkerboard joint, although we knew that it would not be possible to assemble (Figure 30a), and a joint with an apparent checkerboard pattern that can actually be assembled (Figure 30b).

The assemblies were fabricated from 4.5×4.5 cm wooden bars with a 10 mm milling bit. The joint samples were fabricated from 9 cm long pieces of 3.0×3.0 cm wooden bars of light and dark colors; some pieces were painted. Except when otherwise noted, the milling bit size was 6 mm in diameter. We used a Pro Spec Tools 3-axis CNC-milling machine, model

a) Mill bit: Ø 6 mm   b) Mill bit: Ø 10 mm

Figure 28. Two same joint geometries fabricated with differently sized milling bits.
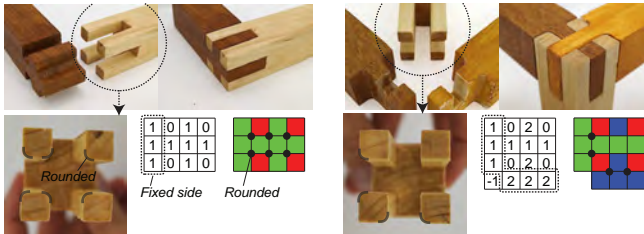
a) Corner rounding 1   b) Corner rounding 2

Figure 29. Two examples of the same geometry of one timber with different rounding of outer corners due to the different organization of intersecting timbers.
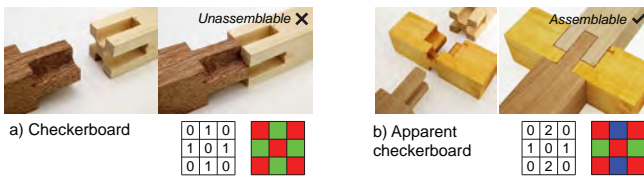

a) Checkerboard   b) Apparent checkerboard

Figure 30. Fabricated examples of true (a) and apparent (b) checkerboard pattern joints.

PSF240. The milling time ranged between 12 and 25 minutes per timber, depending on the joint geometry and wood dimension. The margin of error for manually setting the machine origin was handled by inputting a slightly smaller width compared to the real piece of material, and by sanding the sides after assembling the joint.

LIMITATIONS AND FUTURE WORK

Tsugite focuses on the design of a single joint. In the future, it would be helpful to integrate the design process of the overall structure. Furthermore, this current implementation supports joints with one sliding axis. It is not possible to set individual sliding axes for each timber, which would provide more solutions for 3–6 timber joints (Figure 31a). A CNC machine with 4 or more axes of motion can resolve some sliding limitations, but it would require another set of rules and it is left as future work. In addition, although it is possible to fabricate joints with nonsquare cross-sections, the system is meant for frame structures rather than plate structures (Figure 31b). Most principles could be extended to plate connections by considering other proportions of voxel resolutions and additional functions such as tiling. The main technical difference, however, is that plates have one dominant stable position: lying flat. Therefore, it would be reasonable to allow only for flat material positioning during fabrication, which has implications for fabrication and sliding constraints. Furthermore, the joint geometries of

Tsugite are limited to voxels, and it is not possible to angle arbitrary faces. Owing to this limitation, we cannot create the popular dovetail joint (Figure 31c). It would be interesting future work to cover a larger geometrical design space in the system.
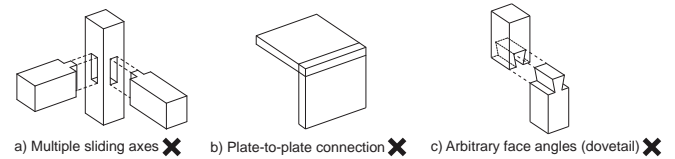

a) Multiple sliding axes ✖   b) Plate-to-plate connection ✖   c) Arbitrary face angles (dovetail) ✖

Figure 31. Limitations.

In addition, there is possibility of reducing computation times by GPU calculation or multi-threading, thereby enabling interactive speeds and gallery search for higher resolution joints. Further, there is an exciting possibility to improve the navigability of the gallery. Currently, joints are sorted by friction or contact area. The grouping of similar joints and interactive tree search could further help users to navigate the space of valid joints. Moreover, we show with an example (Figure 23) that it is possible to create an interlocking assembly with our system, but the global arrangement is not automated. Precedent work have automated the creation of interlocking assemblies [13, 18], but they do not consider the constraints for CNC fabricability and other performances presented in this work. Thus, there is a potential for future work to combine the two systems. Another direction for future work is to perform topological optimization for the structural performance of the joint. This is challenging because FEA is computationally costly and unreliable since the contact points between the timbers might vary greatly with small changes.

However, in reality, the behavior of a joint is very complex. Craftsmen consider metrics beyond the properties that we and other researchers have explored. These include deformation caused by fluctuations of water content and the density of growth rings. These complexities are beyond the scope of this model and any existing computational model of joint and wood behavior. Computers still have a long way to go before being able to match the skill of experienced wood artisans.

ACKNOWLEDGMENTS

REFERENCES

[1] Patrick Baudisch, Arthur Silber, Yannis Kommana, Milan Gruner, Ludwig Wall, Kevin Reuss, Lukas Heilman, Robert Kovacs, Daniel Rechlitz, and Thijs Roumen. 2019. Kyub: A 3D Editor for Modeling Sturdy Laser-Cut Objects. In *Proceedings of the 2019 CHI Conference on Human Factors in Computing Systems (CHI '19)*. ACM, New York, NY, USA, Article 566, 12 pages. DOI:http://dx.doi.org/10.1145/3290605.3300796

[2] Chi-Wing Fu, Peng Song, Xiaoqi Yan, Lee Wei Yang, Pradeep Kumar Jayaraman, and Daniel Cohen-Or. 2015.

Computational Interlocking Furniture Assembly. *ACM Trans. Graph.* 34, 4, Article 91 (July 2015), 11 pages. DOI:`http://dx.doi.org/10.1145/2766892`

[3] Jochen Gros. 2020. 50 Digital Wood Joints by Jochen Gros. (2020). `http://winterdienst.info/50-digital-wood-joints-by-jochen-gros/`

[4] Alec Jacobson. 2019. RodSteward: A Design-to-Assembly System for Fabrication using 3D-Printed Joints and Precision-Cut Rods. *Computer Graphics Forum* (2019).

[5] Kenji Kanasaki and Hiroya Tanaka. 2013. Traditional Wood Joint System in Digital Fabrication. *Computation and Performance - Proceedings of the 31st eCAADe Conference* 1 (2013), 711–717. `http://resolver.tudelft.nl/uuid:d36152ad-7cfc-44b6-bdfe-654f159a3e65`

[6] Robert Kovacs, Anna Seufert, Ludwig Wilhelm Wall, Hsiang-Ting Chen, Florian Meinel, Willi Müller, Sijing You, Yannis Kommana, and Patrick Baudisch. 2017. Demonstrating TrussFab: Fabricating Sturdy Large-Scale Structures on Desktop 3D Printers. (2017), 445–448. DOI:`http://dx.doi.org/10.1145/3027063.3050427`

[7] Maria Larsson, Hironori Yoshida, and Takeo Igarashi. 2019. Human-in-the-loop Fabrication of 3D Surfaces with Natural Tree Branches. In *Proceedings of the ACM Symposium on Computational Fabrication (SCF '19)*. ACM, New York, NY, USA, Article 1, 12 pages. DOI:`http://dx.doi.org/10.1145/3328939.3329000`

[8] Danny Leen, Tom Veuskens, Kris Luyten, and Raf Ramakers. 2019. JigFab: Computational Fabrication of Constraints to Facilitate Woodworking with Power Tools. In *Proceedings of the 2019 CHI Conference on Human Factors in Computing Systems (CHI '19)*. ACM, New York, NY, USA, Article 156, 12 pages. DOI:`http://dx.doi.org/10.1145/3290605.3300386`

[9] Yijing Li and Jernej Barbič. 2014. Stable Orthotropic Materials. In *Proceedings of the ACM SIGGRAPH/Eurographics Symposium on Computer Animation (SCA '14)*. Eurographics Association, Aire-la-Ville, Switzerland, Switzerland, 41–46. `http://dl.acm.org/citation.cfm?id=2849517.2849524`

[10] Shiran Magrisso, Moran Mizrahi, and Amit Zoran. 2018. Digital Joinery For Hybrid Carpentry. In *Proceedings of the 2018 CHI Conference on Human Factors in Computing Systems (CHI '18)*. ACM, New York, NY, USA, Article 167, 11 pages. DOI:`http://dx.doi.org/10.1145/3173574.3173741`

[11] Saigopal Nelaturi, Gregory Burton, Christian Fritz, and Tolga Kurtoglu. 2015. Automatic Spatial Planning for Machining Operations. In *Proceedings of The eleventh annual IEEE International Conference on Automation Science and Engineering (IEEE CASE 2015)*. Gothenburg, Sweden. `nel-bur-fri-kur-case2015.pdf`

[12] Robert J. Ross. 2010. *Wood handbook—Wood as an engineering material*. Department of Agriculture, Forest Service, Forest Products Laboratory.

[13] Peng Song, Chi-Wing Fu, and Daniel Cohen-Or. 2012. Recursive Interlocking Puzzles. *ACM Transactions on Graphics (SIGGRAPH Asia 2012)* 31, 6 (December 2012), 128:1–128:10.

[14] Peng Song, Chi-Wing Fu, Yueming Jin, Hongfei Xu, Ligang Liu, Pheng-Ann Heng, and Daniel Cohen-Or. 2017. Reconfigurable Interlocking Furniture. *ACM Trans. Graph.* 36, 6, Article 174 (Nov. 2017), 14 pages. DOI:`http://dx.doi.org/10.1145/3130800.3130803`

[15] Rundong Tian, Sarah Sterman, Ethan Chiou, Jeremy Warner, and Eric Paulos. 2018. MatchSticks: Woodworking Through Improvisational Digital Fabrication. In *Proceedings of the 2018 CHI Conference on Human Factors in Computing Systems (CHI '18)*. ACM, New York, NY, USA, Article 149, 12 pages. DOI:`http://dx.doi.org/10.1145/3173574.3173723`

[16] Nobuyuki Umetani, Takeo Igarashi, and Niloy J. Mitra. 2012. Guided Exploration of Physically Valid Shapes for Furniture Design. *ACM Trans. Graph.* 31, 4, Article Article 86 (July 2012), 11 pages. DOI:`http://dx.doi.org/10.1145/2185520.2185582`

[17] Nobuyuki Umetani and Ryan Schmidt. 2013. Cross-sectional Structural Analysis for 3D Printing Optimization. In *SIGGRAPH Asia 2013 Technical Briefs (SA '13)*. ACM, New York, NY, USA, Article 5, 4 pages. DOI:`http://dx.doi.org/10.1145/2542355.2542361`

[18] Ziqi Wang, Peng Song, and Mark Pauly. 2018. DESIA: A General Framework for Designing Interlocking Assemblies. *ACM Trans. Graph.* 37, 6, Article 191 (Dec. 2018), 14 pages. DOI:`http://dx.doi.org/10.1145/3272127.3275034`

[19] Chenming Wu, Haisen Zhao, Chandrakana Nandi, Jeffrey I. Lipton, Zachary Tatlock, and Adriana Schulz. 2019. Carpentry Compiler. *ACM Trans. Graph.* 38, 6, Article Article 195 (Nov. 2019), 14 pages. DOI:`http://dx.doi.org/10.1145/3355089.3356518`

[20] Yuan Chieh Yang. 2016. Classical Through Digital. (2016). `https://space10.com/project/classical-through-digital/`

[21] Jiaxian Yao, Danny M. Kaufman, Yotam Gingold, and Maneesh Agrawala. 2017. Interactive Design and Stability Analysis of Decorative Joinery for Furniture. *ACM Trans. Graph.* 36, 2, Article 157a (March 2017). DOI:`http://dx.doi.org/10.1145/3054740`

[22] Hironori Yoshida, Maria Larsson, and Takeo Igarashi. 2019. Upcycling Tree Branches As Architectural Elements Through Collaborative Design and Fabrication. In *Proceedings of the Thirteenth International Conference on Tangible, Embedded, and Embodied Interaction (TEI '19)*. ACM, New York, NY, USA, 589–593. DOI:`http://dx.doi.org/10.1145/3294109.3295639`